Journal of Biochemistry and Molecular Biology, Vol. 40, No. 2, March 2007, pp. 261-269

JOURNAL OF Biochemistry and Molecular Biology

NMR Spectroscopic Assessment of the Structure and Dynamic Properties of an Amphibian Antimicrobial Peptide (Gaegurin 4) Bound to SDS Micelles

SangHo Park[1,2], Woo-Sung Son[2], Yong-Jin Kim[2], Ae-Ran Kwon[2] and Bong-Jin Lee[2,*]

[1]Department of Chemistry and Biochemistry, University of California, San Diego, La Jolla, CA 92093, USA

[2]Research Institute of Pharmaceutical Sciences, College of Pharmacy, Seoul National University, San 56-1, Shillim-dong, Gwanak-gu, Seoul 151-742, Republic of Korea

Received 18 September 2006, Accepted 29 November 2006

The structure and dynamics of a 37-residue antimicrobial peptide gaegurin 4 (GGN4) isolated from the skin of the native Korean frog, *Rana rugosa*, was determined in SDS micelles by NMR spectroscopy. The solution structure of the peptide in SDS micelles was determined from 352 NOE-derived distance constraints and 22 backbone torsion angle constraints. Dynamic properties for the amide backbone were characterized by ^{1}H-^{15}N heteronuclear NOE experiments. The structural study revealed two amphipathic helices spanning residues 2-10 and 16-32 and that the helices were connected by a flexible loop. An intra-residue disulfide bridge was formed between residues Cys31 and Cys37 near the C-terminus. The loop region (11-15) connecting the two helices are were slightly more flexible than these helices themselves. From the fact that since there is no contact NOEs between two helices, it is implied that the GGN4 peptide shows an independent motion of both helices which has an angle of about 60°-120° from each other.

Keywords: Antimicrobial peptide, Dynamics, Gaegurin, Micelle, NMR, Structure

Introduction

Antimicrobial peptides have been attributed pivotal roles in innate immune responses of living organisms (Gabay, 1994). Many different families of antimicrobial peptides, as based on their amino acid sequence and secondary structure, have been isolated from insects, plants, animals, and microorganisms (Boman, 1995; Nicolas and Mor, 1995). In particular, several peptides from the skin of the amphibian have been found to possess broad-spectrum antimicrobial activities (Zasloff, 1987; Gibson *et al.*, 1991; Mor *et al.*, 1991; Simmaco *et al.*, 1991; Morikawa *et al.*, 1992; Simmaco *et al.*, 1993; Clark *et al.*, 1994). Thus, antimicrobial peptides are a promising source of new antibiotics for combating the increasing emergence of drug-resistant bacteria.

Gaegurins (GGNs) have been isolated from the skin of the native Korean frog *Rana rugosa*. These peptides show a broad spectrum of antimicrobial activity against various microorganisms but they appear to have little to no hemolytic properties (Simmaco *et al.*, 1991). The GGNs are divided into two families based upon their amino acid sequence. Thus, Family I includes GGN1 to GGN4, which are composed of 33 to 37 amino acids whereas Family II includes GGN5 and GGN6, which consist of 24 amino acids and contain proline at position 14 near the center of the sequence. All six GGN peptides contain two invariant cysteine residues, one at the C-terminus and the other at position 7 from the C-terminus. The heptapeptide motif containing these two cysteine residues is linked by an intra-residue disulfide bridge, which has been conserved in the antimicrobial peptides derived from other genus *Rana* such as the brevinins, esculentins and ranalexin (Zasloff, 1987; Morikawa *et al.*, 1992; Simmaco *et al.*, 1993). Of the six GGN peptides, GGN4 is most abundant in the frog skin and is believed to play the most important role in the innate defense system of the frog (Park *et al.*, 1994).

Antimicrobial peptides, which adopt one or two amphipathic helices and act directly on the membrane of their target cells, have been studied in different chemical environments: organic solvent-water mixtures, detergent micelles, and lipid bilayers (Bechinger *et al.*, 1993; Gesell *et al.*, 1997; Vignal *et al.*, 1998; Park *et al.*, 2000; Park *et al.*, 2002; Won *et al.*, 2002). It has been reported that the structure of several membrane binding peptides determined in organic solvents are similar to those that have been determined in detergent micelles (Gesell *et al.*, 1997; Vignal *et al.*, 1998; Won *et al.*, 2002). Although

*To whom correspondence should be addressed.
Tel: 82-2-880-7869; Fax: 82-2-872-3632
E-mail: lbj@nmr.snu.ac.kr

organic solvents mimic membrane environments and generally induce the structure of membrane binding proteins and peptides, detergent micelles are regarded as a more adequate environment for membrane binding proteins. Since actual membranes consist of lipid bilayers to form a heterogeneous environment in which their outer head group is polar and their inner acyl group is apolar, detergent micelles can also provide heterogeneous environments characterized by polar head groups and apolar acyl tails. The relatively recent development and application of multidimensional NMR spectroscopy for studies of membrane peptides and proteins takes advantage of the well characterized model membrane environments of detergent micelles (Gesell *et al.*, 1997; Vignal *et al.*, 1998; Park *et al.*, 2002; Won *et al.*, 2002; Leetachewa *et al.*, 2006). Detergent micelles that have been widely used in solution NMR studies of membrane proteins include sodium dodecyl sulfate (SDS), dodecylphosphocholine (DPC), and dihexanoyl-phosphatidylcholine (DHPC).

We have determined the structure of the GGN4 peptide bound to SDS micelles using heteronuclear NMR spectroscopy and compared that to GGN4 binding in a 50% trifluoroethanol (TFE) solution which had been reported previously (Park *et al.*, 2000). Since GGN4 in 50% TFE solution revealed an undefined flexible loop region connecting the two helices, we investigated the backbone dynamics of GGN4 when bound to SDS micelles by using steady-state ^{1}H-^{15}N NOE values. We propose that these results may provide more precise information on the elucidation and understanding of structure-activity relationships of the GGN4 peptide.

Materials and Methods

Materials. $^{15}NH_4Cl$ was obtained from Isotec (Miamisburg) while SDS-d_{25} and DL-1, 4-dithiothreitol-d_{10} were purchased from Cambridge Isotope. 99.95% D_2O, thrombin, carboxypeptidase Y, and phenylmethylsulfonyl fluoride (PMSF) were obtained from Sigma. Sodium 4,4-dimethyl-4-silapentane-1-sulfonate (DSS) was obtained from Aldrich. All other chemicals were analytical grade and were obtained from several different manufacturers.

Sample preparation. The *E. coli* strain DH5α containing the plasmid encoding GST-fused GGN4 was grown in tryptone broth with glucose (TBG) to yield non-labeled GGN4. Uniformly ^{15}N labeled GGN4 was obtained by growing the bacteria in M9 minimal media with $^{15}NH_4Cl$ as the sole nitrogen source. For ^{15}N-Leu and ^{15}N-Lys selectively labeled GGN4 samples, the medium was supplemented with 200 mg/l of each of the 19 amino acids except for 100 mg/l of the desired ^{15}N-labeled amino acid. The purification method used for GGN4 was slightly modified from that cited previously (Park *et al.*, 1994; Park *et al.*, 2000). In brief, suspended in 50 ml of 0.5 M NaCl, 20 mM Tris-HCl (pH 8.0), per liter of culture and disrupted by sonication (duty cycle 30%, output control 5, Branson Sonifier 450) for 10 min on ice, and then centrifuged at 20,000 × *g* for 30 min at 4°C. The supernatant was discarded and the pellet resuspended in a binding buffer (0.5 M NaCl, 5 mM imidazole, 20 mM Tris-HCl, 0.5% sarkosyl, pH 8.0). The fusion protein was cleaved by exposure to a final concentration of 10 μM thrombin for a period of 12 h at 30°C. The resulting His-tagged GGN4 was purified using nickel affinity chromatography (His · Bind Resin) followed by lyophilization. The resulting white powder (His-tagged GGN4) was dissolved in 70% formic acid to a final concentration of 10 mg/ml, and then a 10-fold molar excess of cyanogen bromide (CNBr) was added to the solution. The reaction was kept in the dark for 24 h at room temperature and the reaction mixture then evaporated to dryness and subsequently dissolved in a 95% water/5% acetonitrile mixture. The recombinant GGN4 was purified by semi-preparative reverse-phase HPLC on a Lichrospher C18 column (10 μ, 100Å, 4 × 250 nm, Merck) using a water-acetonitrile gradient. The purity and the primary structure of GGN4 were confirmed by SDS-PAGE (Fig. 1) and matrix-assisted laser desorption/ionization (MALDI) mass spectroscopy. GGN4 prepared by this method yielded a peptide with the same bioactivity as GGN4 isolated directly from frog skin.

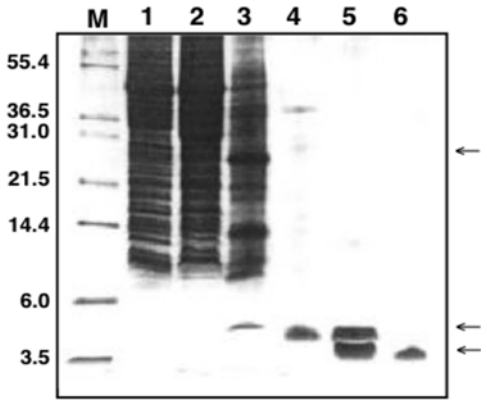

Fig. 1. Protein fractions at different stages of the purification protocol of GGN4 visualized by 15% tricine gel electrophoresis. Lane 1: total cell before IPTG induction, Lane 2: total cell after IPTG induction with the fusion peptide band at 31 kDa. Lane 3: mixture after thrombin digestion, Lane 4: His-tagged GGN4 purified by Ni-affinity chromatography, Lane 5: mixture after CNBr cleavage, Lane 6: purified GGN4 by RP-HPLC. The arrow indicates the band of GST, His-tagged GGN4, and GGN4 from top to bottom.

NMR spectroscopy. All NMR experiments were performed on Bruker DRX 500 and 600 MHz spectrometers equipped with a gradient unit (Park *et al.*, 2003). Samples for NMR measurements were prepared from lyophilized preparations so as to make a 2.0 mM solution in 500 mM SDS-d_{25} (90% H_2O, 10% D_2O), pH 3.0. The ^{1}H-^{15}N HSQC spectra were monitored over an increasing temperature range (from 30°C to 60°C by 5 degree increments). Maximal spectral resolution was obtained at 50°C; therefore, subsequent NMR experiments were performed at 50°C (Fig. 2). A 3-dimensional (3D) ^{15}N-edited TOCSY-HSQC spectrum was recorded with an isotropic mixing time of 60 ms and 3D ^{15}N-edited NOESY-HSQC spectra with 150 and 250 ms mixing times. Water resonance was suppressed by using a WATERGATE sequence. Slowly exchanging amide protons were monitored with a series of ^{1}H-^{15}N HSQC spectra. The $^{3}J_{HNH\alpha}$ coupling constants were measured

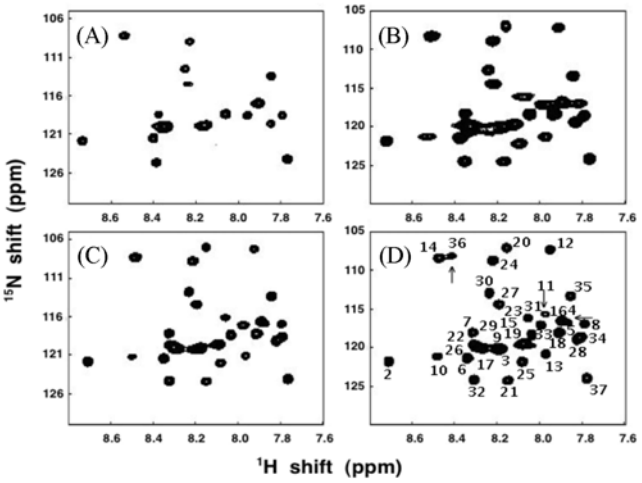

Fig. 2. ^{1}H-^{15}N HSQC spectra of GGN4 in 500 mM SDS micelles monitored at different temperatures. (A) 35°C, (B) 40°C, (C) 45°C, (D) 50°C. Several peaks resolved at 50°C are indicated by the arrows.

from the 2D HMQC-*J* experiment (Kay and Bax, 1990). The ^{1}H-^{15}N steady-state NOE values were determined from spectra recorded in the presence and absence of a proton presaturation period of 3 s (Farrow *et al.*, 1994). ^{1}H saturation was achieved with the use of 120° ^{1}H pulses applied every 5 ms. In the case of the no NOE spectra (equilibrium nitrogen magnetization spectra), a net relaxation delay of 5 s was employed, while a relaxation delay of 2 s prior to a 3 s proton presaturation period was employed for the NOE spectra. The 2D TOCSY, NOESY, and DQF-COSY spectra were also acquired for a non-labeled sample. The 2D TOCSY spectra were acquired using an MLEV-17 spin lock sequence with isotropic mixing times of 30 and 60 ms, respectively. The NOESY spectra were acquired with mixing times of 150, 200, and 250 ms, respectively. For the DQF-COSY experiments, solvent suppression was achieved using selective low-power irradiation of the water resonance. Solvent suppression for the NOESY and TOCSY experiments was achieved by using the WATERGATE sequence. The spectra were processed on a Silicon Graphics Indigo-2 workstation, using the NMRPipe program (Delaglio *et al.*, 1995). Chemical shifts were referenced to the methyl signal of DSS.

Structure calculations. Distance restraints were obtained from the homonuclear and heteronuclear NOESY spectra with 200 ms mixing times. Comparisons were made to the 150 and 250 ms NOESY spectra to assess possible contributions from spin diffusion. All NOE data were classified into three classes: strong, medium, and weak, corresponding to upper bound interproton distance restraints of 3.0, 4.0, and 5.0 Å, respectively. Lower distance bounds were taken as the sum of the van der Waals radii of 1.8 Å. As no stereospecific assignment could be made for the methyl and methylene protons, appropriate pseudo atom corrections were applied (Wüthrich *et al.*, 1983). A total of 352 NOE constraints, 22 backbone dihedral angle restraints, and 28 hydrogen bond restraints were included in the calculation of the structures. In addition, three other restraints were added to define the disulfide bridge between Cys31 and Cys37. Thus, the target values of S(31)-S(37), S(31)-C(37), and S(37)-C(31) were set to 2.20 (± 0.02) Å, 2.99 (± 0.5) Å, and 2.99 (± 0.5) Å, respectively (Nilges *et al.*, 1988).

The structure calculations of the peptides were performed using repeated iterative cycles of *ab initio* simulated annealing using the force field adapted for NMR structure determination (parallhdg.pro) in XPLOR 3.851 (Brünger, 1992). Simulated annealing was performed from an extended conformation for 30 ps (time step = 5 fs) with an initial annealing temperature of 1,000 K, which was followed by 15 ps (time step = 5 fs) cooling steps to 100 K. Refinement of the structures was performed using the conjugate gradient Powell algorithm with an initial annealing temperature of 300 K and 5,000 cycles of energy minimization, using the same force field file (parallhdg.pro) with *ab initio* simulated annealing protocol. A total of 48 structures of the peptides, with no distance violation larger than 0.5 Å and no dihedral violation larger than 5°, were accepted from the 50 structures that were generated. The 20 best structures of the peptides determined on the basis of their total energy and with no systematic distance violation greater than 0.3 Å and no dihedral angle violation larger than 3° were selected as the final structures of the peptides.

Results

Purification of GGN4. The overexpression of a protein is a prerequisite for efficient heteronuclear NMR studies, however, it is difficult to over express GGN4 directly in *E. coli* due to the innate toxicity towards the microbe. To obtain the relatively large quantities of peptide needed and produce the peptide without killing the *E. coli*, GGN4 was constructed and expressed as a fusion peptide utilizing the glutathione-S-transferase (GST)-fusion system (Park *et al.*, 1994). The GST-GGN4 fusion protein was successfully over expressed in *E. coli* (Fig. 1, lane 1 and 2) and subsequently purified efficiently as inclusion bodies. After thrombin directed cleavage of the fusion protein, His-tagged GGN4 was purified by Ni affinity chromatography and then cleaved with CNBr to release intact GGN4 peptide (Fig. 1, lanes 3-6). Typically, 2 mg of GGN4 could be obtained from 1L of cell culture in uniformly ^{15}N labeled minimal media. The homogeneity of the purified peptide was confirmed by MALDI TOF mass spectroscopy.

NMR spectroscopy of GGN4 in SDS micelles. On the basis of the assignment results of GGN4 previously obtained in a 50% TFE solution (Park *et al.*, 2000), the assignment of backbone atoms of GGN4 in SDS micelles was mainly performed by conducting the heteronuclear experiments in combination with the method proposed by Wüthirch (Wüthrich, 1986). Since the molecular weight of GGN4 bound to SDS micelles increased to about 25 kDa, the overall NMR signals were broadened when compared to the signals in a 50% TFE solution so that several peaks overlapped. To optimize the spectral resolution, we monitored the ^{1}H-^{15}N HSQC spectra of GGN4 in SDS micelles by 5 degree step-wise increments of temperature (from 30°C to 60°C) (Fig. 2). We achieved maximal spectral resolution at 50°C whereby the appropriate number of backbone and side chain resonances were present

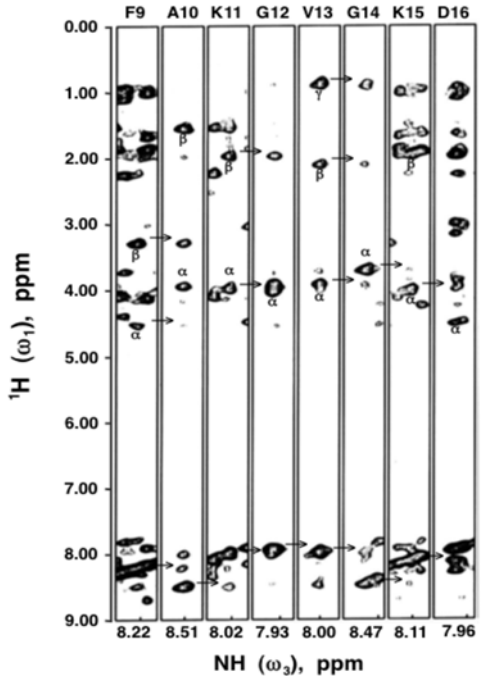

Fig. 3. Series of strips selected from a 3D ^{1}H-^{15}N NOESY-HSQC spectrum of GGN4 in the 500 mM SDS micelles. The spectrum was recorded at 50°C with a mixing time of 200 ms and extracted at the ^{15}N chemical shifts of residues Phe9 to Asp16. Intra-residual contacts are labeled with symbols. Sequential NOE contacts are represented by arrows.

without evidence of resonance doubling indicative of multiple species contributing to conformational heterogeneity (Fig. 2D). Although there is limited dispersion in the ^{1}H chemical shift dimension typical of a helical peptide, all of the backbone resonances were resolved and assigned as indicated.

The sequential connections were compared with $d_{\alpha N}$ (i, $i+3$), $d_{\alpha N}$ (i, i+4), and $d_{\alpha\beta}$(i, i+3) connections to ensure their assignments. Assignment ambiguities due to peak overlaps were resolved by selectively using ^{15}N Leu and Lys labeled samples of the ^{1}H-^{15}N HSQC spectra. Figure 3 demonstrates ^{1}H(ω_1), NH(ω_3) cross sections obtained from a 3D ^{1}H-^{15}N NOESY-HSQC spectrum of GGN4 extracted at different ^{15}N amide frequencies (ω_2). The sequential connection was represented from residues Phe9 to Asp16, which contained the flexible loop region (Lys11-Lys15). The chemical shift values of proton and ^{15}N resonances of GGN4 in a 500 mM SDS micelle are presented in Table 1.

The short and medium inter-residue NOE cross-peaks identified by this study and their relative intensities are presented in Fig. 4. The NOE connectivity's of GGN4 in SDS micelles are similar with those cited for the 50% TFE solution. This observation indicates nearly complete sets of d_{NN} (i, $i+1$), $d_{\alpha\beta}$(i, $i+3$), $d_{\alpha N}$ (i, $i+4$), and $d_{\alpha N}$ (i, $i+3$) NOE connectivities for residues 2 to 10 and 16 to 32, and suggests the presence of a regular α-helical conformation. $^3J_{HNH\alpha}$ coupling constants for residues 2-10 and 16-32 show almost less than 5.5 Hz except for the residues, Gln8, Phe9, Gly20, Gly24, and Cys31. Further support for helical regions to exist between residues 2-10 and 16-32 was provided by the amide proton exchange data. Slowly exchanging amide protons were observed in the central residues of the helical segments spanning residues 6-10 and 20-32. The chemical shifts of the α-protons of residues 2-10 and 16-32 showed an overall up field shift tendency by 0.1 to 0.4 ppm compared to random coil chemical shifts, which also supports the notion of the helical conformation of GGN4 (Wishart *et al.*, 1992). The intra-residue disulfide bond between Cys31 and Cys37 can be inferred from the presence of the NOE cross-peaks of Cys31H$_\beta$-Cys37H$_\beta$, Cys31NH-Cys37H$_\beta$, and Cys31H$_\beta$-Cys37NH.

Three-dimensional structure and dynamic properties. A set of 50 structures of GGN4 was calculated by using 352 distance restraints, 22 dihedral angle restraints, and 28 hydrogen bond restraints. Simulated annealing (SA) calculations were performed to produce structures with a common fold that were in acceptable agreement with the experimental restraints and with low total energies. Of the 50 structures, 48 with no distance violation greater than 0.5 and no dihedral violation larger than 5° were selected. The 20 structures with the lowest energies were then chosen to represent the solution structure of the GGN4 peptide. Among these 20 structures, three were considered as representative and were depicted by two locally well-defined helices comprised of residues 2 to 10 on one hand and residues 16 to 32 on the other (Fig. 5). The 20 structures chosen revealed that there is no contact between the helices thereby allowing an independent movement of both helices at an angle of 60°-120° to each other.

The dynamic behavior of the GGN4 peptide bound to SDS micelles was probed by the heteronuclear ^{1}H-^{15}N NOE experiment. The experimental ^{1}H-^{15}N heteronuclear NOEs for all backbone amide sites of the membrane-bound GGN4 are shown in Fig. 6. The regions with the longest correlation times, as reflected in the positive ^{1}H-^{15}N heteronuclear NOE values, generally correlated with the locations of the helices. The N- and C-terminal residues are substantially more flexible than are the residues within the helices. The loop region (11-15) connecting the two helices are slightly more flexible than the helices.

Structural statistics for the mean and 20 converged structures were evaluated in terms of structural parameters (Table 2). The 20 final converged structures were shown to exhibit an RMSD about the mean coordinate positions for residues 2-10 and for residues 16-32 and were 0.21 and 0.61 for their backbone atoms, respectively.

Table 1. ^{1}H and ^{15}N resonance assignment of GGN4 in 500 mM SDS micelles at 50°C, pH 3.0

Residue	^{15}N	HN	αH	βH	γH	others
Gly1						
Ile2	125.6	8.71	4.09	1.99	1.66, 1.34	$\gamma CH_3/\delta CH_3$ 1.02
Leu3	124.1	8.17	4.12	1.86, 1.86	1.68	δCH_3 1.01, 1.01
Asp4	120.3	7.92	4.49	3.03, 3.03		
Thr5	122.1	7.92	4.05	4.35	1.27	
Leu6	125.3	8.33	4.18	1.97, 1.97	1.70	δCH_3 0.95, 0.95
Lys7	122.1	8.30	3.94	2.03, 2.03	1.72, 1.72	δCH_2 1,45, 1.45
Gln8	120.8	7.80	4.11	2.24, 2.24	NO[b]	δNH_2 7.38, 6.73
Phe9	124.2	8.22	4.55	3.30, 3,30		2,6H/3,5H 7.25, 7.24
Ala10	125.1	8.51	3.94	1.55		
Lys11	119.9	8.02	3.98	1.97, 1.97	1.82, 1.82	δCH_2 1.70, 1.48
Gly12	111.0	7.93	3.98			
Val13	125.0	8.00	3.91	2.11	0.89, 0.89	
Gly14	111.8	8.47	3.71			
Lys15[a]	123.6	8.11	4.01	1.96, 1.96	1.63, 1.63	δCH_2 1.49, 1.49
Asp16	121.0	7.96	4.52	3.16, 2.98		
Leu17	125.0	8.26	4.25	1.95, 1.95	1.64	δCH_3 1.12, 0.94
Val18	121.0	7.95	3.88	2.26	1.09, 0.93	
Lys19[a]	123.6	8.11	4.01	1.96, 1.96	1.63, 1.63	δCH_2 1.49, 1.49
Gly20	110.6	8.16	4.00			
Ala21	128.3	8.19	4.35	1.54		
Ala22	123.6	8.34	4.13	1.54		
Gln23	120.0	8.10	4.10	2.24, 2.24	2.52, 2.52	δNH_2 7.28, 6.80
Gly24	112.6	8.22	4.07			
Val25	125.9	8.11	3.93	2.27	1.14, 1.00	
Leu26	123.7	8.32	4.10	1.87, 1.74	NO	δCH_3 1.11, 0.99
Ser27	118.3	8.21	4.29	4.08, 4.08		
Thr28	122.6	7.83	4.40	4.40	1.29	
Val29	124.2	8.28	3.72	2.26	0.99, 0.99	
Ser30	117.0	8.26	4.15	4.03, 4.03		
Cys31	122.2	8.03	4.68	3.49, 3.14		
Lys32	127.8	8.29	4.25	2.15, 1.89	1.69, 1.55	NO
Leu33	123.1	8.05	4.25	1.91, 1.91	1.63	δCH_3 0.96, 0.96
Ala34	122.5	7.82	4.40	1.57		
Lys35	117.3	7.85	4.22	2.24, 2.06	1.80, 1.52	NO
Thr36	112.4	8.40	4.53	4.22	1.19	
Cys37	126.7	7.82	4.71	3.72, 3.03		

[a]Overlap between K15 and K19; [b]NO, not observed

Discussion

As a result of this study, we have been able to determine the structure of the GGN4 peptide in SDS micelles. Insofar detergent micelles are regarded as appropriate materials than organic solvents for studying membrane peptides and proteins by solution NMR spectroscopy (Nelson and Kallenbach, 1986; Park *et al.*, 2002; Roccatano *et al.*, 2002; Maeda *et al.*, 2003).

The structure of GGN4 in SDS micelles was shown to be similar to that using 50% TFE solvents. Our results are also in agreement with the CD studies of GGN4 showing that the peptide forms mainly an α-helix in 50% TFE/water solvents, DPC micelles, and SDS micelles, and that the helix content estimated under these conditions almost same to be about 70% (Park *et al.*, 2000). Alternatively, GGN5 another antimicrobial peptide (of the Family II of GGN) and several of its derivatives, have a 5-10% higher helix content in 50% TFE/water solvents than in SDS and DPC micelles which suggests that TFE may induce or stabilize helical structures (Park *et al.*, 2002). However, determination of their structures by NMR spectroscopy in SDS micelles showed a more helical

Fig. 4. Summary of the NOE connectivity's, $^3J_{HNH\alpha}$ coupling constants, amide proton exchange rates, and the chemical shift index (CSI) of GGN4 in 500 mM SDS micelles. Small (<5.5 Hz) coupling constants and a CSI value of -1 are represented as filled circles. Fast, moderate, and slow exchange amides are represented as open, gray, and filled circles, respectively.

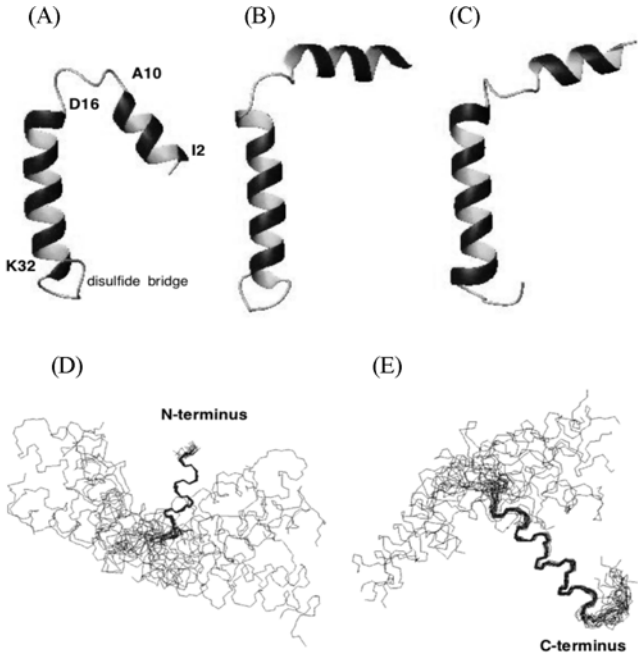

Fig. 5. Three representative structures of GGN4 determined in SDS micelles. These structures were selected from 20 of the lowest-energy structures. Both helices are located at angles of about (A) 60°, (B) 90°, and (C) 120° to each other. The structures of GGN4 are presented and were aligned for the best overlap of residues (D) 2-10 (RMSD of backbone atom = 0.208) (E) 16-32 (RMSD of backbone atom = 0.610), respectively.

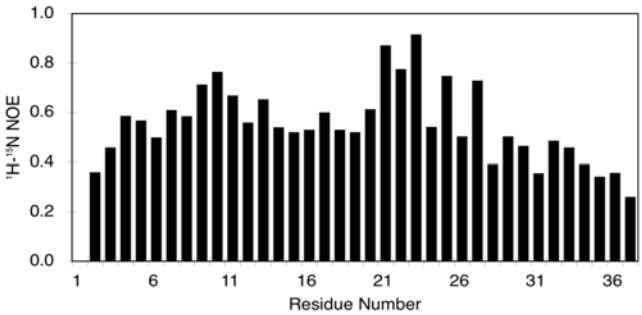

Fig. 6. ^{15}N relaxation parameter of steady-state ^{1}H-^{15}N heteronuclear NOE of GGN4 in 500 mM SDS micelles as a function of the residue number.

propensity than estimated from CD spectroscopy. In the case of maganin and ranalexin, their structures were shown to be very similar in both mixed organic solvents and detergent micelles (Gesell *et al.*, 1997; Vignal *et al.*, 1998). The common features of GGN4, maganin, and ranalexin are their water solubility and adoption of an amphipathic helix in a membrane configuration and to interact primarily with the head groups of lipids, perhaps leading to a similar structure in mixed organic solvents and the detergent micelles.

The structural dynamics data revealed several important insights into the interactions between the GGN4 peptide and the SDS micelles. It is widely recognized that proteins continuously undergo significant internal movement over a wide range of time-scales (Karplus and McCammon, 1986) and a principle motivation for NMR studies of proteins has been the desire to characterize their "solution structure". The solution structure then can be defined as the dynamic aspects of protein architecture. The backbone of the molecule and the dynamics of the molecule are more obviously coupled in proteins that occupy membranes than in other protein classes, and the heteronuclear ^{1}H-^{15}N NOE provides a remarkably direct and sensitive indication of the local dynamics of membrane proteins in micelles (Christensen *et al.*, 1988; Holak *et al.*, 1988; Shon *et al.*, 1991; Almeida and Opella, 1997; Papavoine *et al.*, 1997).

The three-dimensional structure of the GGN4 peptide reveals a poorly defined flexible loop region connecting two helices. Further, the backbone dynamics shows that GGN4 has some degree of internal flexibility. The loop region (11-15) connecting the two helices are slightly more flexible than the helices themselves. In addition, two amphipathic helices probably bound on the surface of the micelles have some motility which may be related to a membrane permeation mechanism.

The overall topology of the secondary structure and the physico-chemical properties of the two helices of GGN4 are similar to those described for cecropin A, a well-known 37-residue antimicrobial peptide isolated from insects and known

Table 2. Structural statistics of GGN4 as determined in 500 mM SDS micelles

Restraints for structure calculations	
Total NOE restraints	352
Intra-residue	147
Sequential (|i - j| = 1)	122
Medium range (1 < |i - j| < 5)	76
Long range (|i - j| > 4)	7
Hydrogen bond restraints[a]	28
Dihedral angle restraints[b]	22
Statistics for structure calculations	
RMSDs from idealized covalent geometry	
Bonds (Å)	0.0011 ± 0.0002
Bond angles (°)	0.441 ± 0.010
Improper torsions (°)	0.345 ± 0.006
RMSDs from exprerimental restraints	
Distances (Å)	0.023 ± 0.002
Final energies (kcal mol^{-1})	
E_{total}	61.4 ± 3.3
E_{bonds}	0.7 ± 0.2
E_{angles}	29.9 ± 1.5
$E_{impropers}$	4.6 ± 0.2
E_{vdW}	16.3 ± 1.6
E_{NOE}	9.8 ± 1.4
Average RMSD to the mean structure for the backbone/ non-H atoms (Å)	
Whole (2-37)	3.24/4.36
N-terminal helix (2-10)	0.21/1.11
C-teminal helix (16-32)	0.61/1.20
loop (11-15)	1.15/2.73
Disulfide bridge (31-37)	0.89/2.05

[a]HN-O, 1.8-2.0Å; N-O, 2.7-3.0Å. [b]Target angle of $-65^{o} \pm 25^{o}$ for below 4.0 Hz and that of $-65^{o} \pm 35^{o}$ for below 5.5 Hz.

to form channels in lipid bilayers (Christensen *et al.*, 1988; Holak *et al.*, 1988; Almeida and Opella, 1997). It has been also reported that GGN4 has an ionophoric activity that could be responsible for antimicrobial properties by forming voltage-dependent and cation-selective pores in the membrane lipid bilayers (Kim *et al.*, 1999). Therefore, we have previously suggested that the mechanism of GGN4 antimicrobial activity is similar to that of the cecropins despite differences in amino-acid sequences and animal origin (Park *et al.*, 2000).

The recent models for membrane permeation mechanisms may explain how the GGN4 peptide forms an ionophore in lipid bilayers (Oren and Shai, 1998). In the 'barrel-stave' mechanism, the transmembrane amphipathic α-helices form bundles and produce a transmembrane pore whereas the 'carpet-like' mechanism describes membrane disintegration by disruption of the bilayers curvature leading to micellization. In this latter model, in contrast to the 'barrel-stave' concept, the peptides do not penetrate into the hydrophobic core of the membrane but rather bind to phospholipids head groups. Based on the electro-chemical data of GGN4 (Kim *et al.*, 1999), it can be suggested that the two amphipathic helices of GGN4 lie in the plane of the bilayers under equilibrium conditions and transiently span the lipid bilayers to form transmembrane pores that are similar to those formed by peptides derived from ionotropic receptors. Therefore, GGN4 may act as the barrel-stave mechanism itself rather than behave as the carpet-like mechanism.

In summary, our results afford further insight into the possible mechanism of action of the GGN4 peptide at the structural level and contribute to improved understanding of the dynamic behavior of GGN4 at a membrane level. In the case of magainin, it has been reported that this peptide can form pores perpendicular to the membrane bilayer at high concentrations (Ludtke *et al.*, 1996).

At present, there is no unequivocal evidence that GGN4 forms a stable oligomer. Complementary experiments are therefore necessary to determine whether GGN4 functions in a monomeric or multimeric manner as well as to characterize the precise orientation and dynamic properties of the two helices of GGN4 in lipid bilayers.

Acknowledgments This work was supported by a National Research Laboratory program (M1-0412-00-0075) from the Korea Institute Science & Technology Evaluation and Planning, Republic of Korea and supported by a fostering project of the Lab of Excellency from the Ministry of Education and Human Resources Development (MOE), the Ministry of Commerce, Industry and Energy (MOCIE) and the Ministry of Labor (MOLAB). In addition, this work was also supported in part by the 2006 BK21 project for Medicine, Dentistry, and Pharmacy. We thank the National Center for Inter-university Research facilities at Seoul National University (NCIRF) and the Korea Basic Science Institute (KBSI) for providing high field NMR equipment.

References

Almeida, F. C. and Opella, S. J. (1997) Fd coat protein structure in membrane environments: structural dynamics of the loop between the hydrophobic trans-membrane helix and the amphipathic in-plane helix. *J. Mol. Biol.* **270**, 481-495.

Bechinger, B., Zasloff, M. and Opella, S. J. (1993) Structure and orientation of the antibiotic peptide magainin in membranes by solid-state nuclear magnetic resonance spectroscopy. *Protein Sci.* **2**, 2077-2084.

Boman, H. G. (1995) Peptide antibiotics and their role in innate immunity. *Annu. Rev. Immunol.* **13**, 61-92.

Brünger, A. T. (1992) *X-PLOR, Version 3.1: a system for X-ray crystallography and NMR*. Yale University Press, New Haven, USA.

Christensen, B., Fink, J., Merrifield, R. B. and Mauzerall, D. (1988) Channel-forming properties of cecropins and related model compounds incorporated into planar lipid membranes. *Proc. Natl. Acad. Sci. USA* **85**, 5072-5076.

Clark, D. P., Durell, S., Maloy, W. L. and Zasloff, M. (1994)

Ranalexin. A novel antimicrobial peptide from bullfrog (Rana catesbeiana) skin, structurally related to the bacterial antibiotic, polymyxin. *J. Biol. Chem.* **269**, 10849-10855.

Delaglio, F., Grzesiek, S., Vuister, G. W., Zhu, G., Pfeifer, J. and Bax, A. (1995) NMRPipe: a multidimensional spectral processing system based on UNIX pipes. *J. Biomol. NMR* **6**, 277-293.

Farrow, N. A., Muhandiram, R., Singer, A. U., Pascal, S. M., Kay, C. M., Gish, G., Shoelson, S. E., Pawson, T., Forman-Kay, J. D. and Kay, L. E. (1994) Backbone dynamics of a free and phosphopeptide-complexed Src homology 2 domain studied by 15N NMR relaxation. *Biochemistry* **33**, 5984-6003.

Gabay, J. E. (1994) Ubiquitous natural antibiotics. *Science* **264**, 373-374.

Gesell, J., Zasloff, M. and Opella, S. J. (1997) Two-dimensional 1H NMR experiments show that the 23-residue magainin antibiotic peptide is an alpha-helix in dodecylphosphocholine micelles, sodium dodecylsulfate micelles, and trifluoroethanol/water solution. *J. Biomol. NMR* **9**, 127-135.

Gibson, B. W., Tang, D. Z., Mandrell, R., Kelly, M. and Spindel, E. R. (1991) Bombinin-like peptides with antimicrobial activity from skin secretions of the Asian toad, *Bombina orientalis*. *J. Biol. Chem.* **266**, 23103-23111.

Holak, T. A., Engstrom, A., Kraulis, P. J., Lindeberg, G., Bennich, H., Jones, T. A., Gronenborn, A. M. and Clore, G. M. (1988) The solution conformation of the antibacterial peptide cecropin A: a nuclear magnetic resonance and dynamical simulated annealing study. *Biochemistry* **27**, 7620-7629.

Karplus, M. and McCammon, J. A. (1986) The dynamics of proteins. *Sci. Am.* **254**, 42-51.

Kay, L. E. and Bax, A. (1990) New methods for the measurement of NH-CaH coupling constants in 15N-labeled proteins. *J. Magn. Reson.* **86**, 110-126.

Kim, H. J., Han, S. K., Park, J. B., Baek, H. J., Lee, B. J. and Ryu, P. D. (1999) Gaegurin 4, a peptide antibiotic of frog skin, forms voltage-dependent channels in planar lipid bilayers. *J. Pept. Res.* **53**, 1-7.

Leetachewa, S., Katzenmeier, G. and Angsuthanasombat, C. (2006) Novel preparation and characterization of the alpha4-loop-alpha5 membrane-perturbing peptide from the *Bacillus thuringiensis* Cry4Ba delta-endotoxin. *J. Biochem. Mol. Biol.* **39**, 270-277.

Ludtke, S. J., He, K., Heller, W. T., Harroun, T. A., Yang, L. and Huang, H. W. (1996) Membrane pores induced by magainin. *Biochemistry* **35**, 13723-13728.

Maeda, Y., Nakagawa, T. and Kuroda, Y. (2003) Oligopeptide-mediated helix stabilization of model peptides in aqueous solution. *J. Pept. Sci.* **9**, 106-113.

Mor, A., Nguyen, V. H., Delfour, A., Migliore-Samour, D. and Nicolas, P. (1991) Isolation, amino acid sequence, and synthesis of dermaseptin, a novel antimicrobial peptide of amphibian skin. *Biochemistry* **30**, 8824-8830.

Morikawa, N., Hagiwara, K. and Nakajima, T. (1992) Brevinin-1 and -2, unique antimicrobial peptides from the skin of the frog, *Rana brevipoda porsa*. *Biochem. Biophys. Res. Commun.* **189**, 184-190.

Nelson, J. W. and Kallenbach, N. R. (1986) Stabilization of the ribonuclease S-peptide alpha-helix by trifluoroethanol. *Proteins* **1**, 211-217.

Nicolas, P. and Mor, A. (1995) Peptides as weapons against microorganisms in the chemical defense system of vertebrates. *Annu. Rev. Microbiol.* **49**, 277-304.

Nilges, M., Gronenborn, A. M., Brunger, A. T. and Clore, G. M. (1988) Determination of three-dimensional structures of proteins by simulated annealing with interproton distance restraints. Application to crambin, potato carboxypeptidase inhibitor and barley serine proteinase inhibitor 2. *Protein Eng.* **2**, 27-38.

Oren, Z. and Shai, Y. (1998) Mode of action of linear amphipathic alpha-helical antimicrobial peptides. *Biopolymers* **47**, 451-463.

Papavoine, C. H., Remerowski, M. L., Horstink, L. M., Konings, R. N., Hilbers, C. W. and van de Ven, F. J. (1997) Backbone dynamics of the major coat protein of bacteriophage M13 in detergent micelles by 15N nuclear magnetic resonance relaxation measurements using the model-free approach and reduced spectral density mapping. *Biochemistry* **36**, 4015-4026.

Park, J. M., Jung, J. E. and Lee, B. J. (1994) Antimicrobial peptides from the skin of a Korean frog, *Rana rugosa*. *Biochem. Biophys. Res. Commun.* **205**, 948-954.

Park, S. H., Kim, H. E., Kim, C. M., Yun, H. J., Choi, E. C. and Lee, B. J. (2002) Role of proline, cysteine and a disulphide bridge in the structure and activity of the anti-microbial peptide gaegurin 5. *Biochem. J.* **368**, 171-182.

Park, S. H., Kim, Y. K., Park, J. W., Lee, B. and Lee, B. J. (2000) Solution structure of the antimicrobial peptide gaegurin 4 by H and 15N nuclear magnetic resonance spectroscopy. *Eur. J. Biochem.* **267**, 2695-2704.

Park, S. J., Kim, J. S., Son, W. S., Ahn, H. C. and Lee, B. J. (2003) Backbone 1H, 15N, and 13C resonance assignments of the *Helicobacter pylori* acyl carrier protein. *J. Biochem. Mol. Biol.* **36**, 505-507.

Roccatano, D., Colombo, G., Fioroni, M. and Mark, A. E. (2002) Mechanism by which 2,2,2-trifluoroethanol/water mixtures stabilize secondary-structure formation in peptides: a molecular dynamics study. *Proc. Natl. Acad. Sci. USA* **99**, 12179-12184.

Shon, K. J., Kim, Y., Colnago, L. A. and Opella, S. J. (1991) NMR studies of the structure and dynamics of membrane-bound bacteriophage Pfl coat protein. *Science* **252**, 1303-1305.

Simmaco, M., Barra, D., Chiarini, F., Noviello, L., Melchiorri, P., Kreil, G. and Richter, K. (1991) A family of bombinin-related peptides from the skin of *Bombina variegata*. *Eur. J. Biochem.* **199**, 217-222.

Simmaco, M., Mignogna, G., Barra, D. and Bossa, F. (1993) Novel antimicrobial peptides from skin secretion of the European frog *Rana esculenta*. *FEBS Lett.* **324**, 159-161.

Vignal, E., Chavanieu, A., Roch, P., Chiche, L., Grassy, G., Calas, B. and Aumelas, A. (1998) Solution structure of the antimicrobial peptide ranalexin and a study of its interaction with perdeuterated dodecylphosphocholine micelles. *Eur. J. Biochem.* **253**, 221-228.

Wishart, D. S., Sykes, B. D. and Richards, F. M. (1992) The chemical shift index: a fast and simple method for the assignment of protein secondary structure through NMR spectroscopy. *Biochemistry* **31**, 1647-1651.

Won, H. S., Park, S. H., Kim, H. E., Hyun, B., Kim, M., Lee, B. J. and Lee, B. J. (2002) Effects of a tryptophanyl substitution on the structure and antimicrobial activity of C-terminally truncated gaegurin 4. *Eur. J. Biochem.* **269**, 4367-4374.

Wüthrich, K. (1986) *NMR of proteins and nucleic acids*. Wiley, New York, USA

Wuthrich, K., Billeter, M. and Braun, W. (1983) Pseudo-structures

for the 20 common amino acids for use in studies of protein conformations by measurements of intramolecular proton-proton distance constraints with nuclear magnetic resonance. *J. Mol. Biol.* **169**, 949-961.

Zasloff, M. (1987) Magainins, a class of antimicrobial peptides from Xenopus skin: isolation, characterization of two active forms, and partial cDNA sequence of a precursor. *Proc. Natl. Acad. Sci. USA* **84**, 5449-5453.